Purinergic Signalling (2016) 12:537–547
DOI 10.1007/s11302-016-9519-2

ORIGINAL ARTICLE

Adenosine A2B receptors play an important role in bone homeostasis

Carmen Corciulo[1] · **Tuere Wilder**[1] · **Bruce N. Cronstein**[1,2]

Received: 22 March 2016 / Accepted: 18 May 2016 / Published online: 11 June 2016

Abstract Bone homeostasis is a finely regulated mechanism involving different molecular pathways including adenosine signaling. The aim of this study is to determine the bone phenotype of adenosine A2B receptor knockout (A2BRKO) mice and to measure their ability to form new bone. Moreover, we analyzed the functionality of osteoclasts and osteoblasts from A2BRKO mice. Microcomputed tomography (μCT) analysis revealed a decrease of bone substance, bone mineral density, and trabecular number in A2BRKO mice compared to the WT mice at the same age. We measured the new bone formation by injecting fluorescent markers: it was reduced in femur and tibia of A2BRKO mice compare to the WT. A2BRKO young mice have fewer osteoblasts and an increase of osteoclasts was measured in the hind limbs of young and adult mice. A2BRKO osteoclasts are also more active in vitro, showing an increase of pit formation in dentin discs. Surprisingly in mature osteoblasts from A2BRKO mice, we measured an increase of calcified matrix production, collagen deposition, and alkaline phosphatase activity. These results demonstrate that A2BR on osteoblasts and osteoclasts regulate bone homeostasis.

Keywords Adenosine A2B · Bone homeostasis · A2BRKO mice

✉ Carmen Corciulo
Carmen.Corciulo@nyumc.org

[1] Division of Translational Medicine, New York, NY, USA

[2] Department of Medicine, Division of Rheumatology, NYU School of Medicine, 550 First Ave, New York, NY 10016, USA

Introduction

The skeleton is a highly dynamic tissue that undergoes constant remodeling and regeneration throughout adult life. Among the many signaling molecules and factors that regulate bone homeostasis is adenosine; adenosine and its four receptors (A1R, A2AR, A2BR, and A3R) are well known to be involved in many physiological and pathological mechanisms, including bone homeostasis [1]. Thus, our laboratory has previously reported that blockade or deletion of A1R leads to increased bone density in mice since endogenous activity of A1R is important in osteoclast formation by bone marrow cells [2–4]. In contrast, A2AR ligation enhances bone regeneration by inhibiting differentiation of osteoclasts and by promoting osteoblast functionality and, when deleted in vivo, leads to a marked reduction in bone density in mice [5–8].

Prior studies indicate that A2BRKO mice display a delay in normal fracture healing [9] and engagement of A2BR has also been reported to play an important role in regulating the differentiation and function of cells involved in bone homeostasis. A2BR engagement stimulates osteoblast differentiation from mesenchymal stem cell precursors [3, 9–13]. Indeed, engagement of A2BR by excess adenosine produced in response to contact with scaffolds containing Ca^{++}phosphate is thought to contribute to the bone healing properties of these scaffolds [13]. In addition, A2BR occupancy suppresses osteoclast differentiation and function as well [3]. Therefore, we examined the effect of A2BR deletion on bone homeostasis. We examined the bone phenotype of A2BR knockout mice from youth through adult life and determined whether there were changes in bone homeostasis and whether they evolved over time in mice lacking A2BR. Moreover, we analyzed the ex vivo functionality of osteoclasts and osteoblasts from A2BRKO mice.

Material and methods

Reagents

Paraformaldehyde (32 %) was purchased from Electron Microscopy Sciences (PA, USA); ethylenediaminetetraacetic acid (EDTA), Naphthol AS-MX phosphate, Fast Red Violet LB salt, bovine serum albumin (BSA), Sigma Fast DAB Tablet Sets, calcein, Alizarin-3-methyliminodiacetic acid, sucrose, gentamicin, amphotericin B, 2-phospho-L-ascorbic acid trisodium salt, Toluidine Blue, Direct Red 80, SIGMA *FAST* BCIP/NBT, and primers (F4/80 (ADGRE) Forward 5′- TGCATCTAGCAATGGACAGC-3′, Reverse 3′- TTCAAATGGATCCAGAAGGC-5′; *CTSK* (CATHEPSIN-K Forward 5′-GCTGAACTCAGGACCTCTGG-3′, Reverse 5′-GAAAAGGGAGGCATGAATGA-3′)) were purchased from Sigma-Aldrich (MO, USA); Rb-Osteopontin antibody was purchased from Abcam (MA, USA); proteinase K was purchased from Promega (CA, USA); FBS, Alpha-MEM, MuLV Reverse transcriptase, Rnase Inhibitor, and Random hexamers dNTPs were purchased from Life technology (NY, USA); penicillin/streptomycin was obtained from Invitrogen (NY, USA); Goat anti-rabbit HRP-conjugate antibody was bought from Santa-Cruz (CA, USA); Recombinant Mouse M-CSF Protein (MCSF) and Recombinant Mouse TRANCE/RANK L/TNFSF11 were purchased from R&D (MN, USA); collagenase type II was from Worthington, Brilliant III ultra-fast SYBR Green QPCR master mix from Agilent (CA, USA), and RNeasy mini kit and Qiashredder columns from Qiagen (CA, USA).

Animals

Mice employed in this study were kept under regular lighting conditions (12 h light/dark cycles) and given food and water ad libitum. Adenosine A2B receptor knockout (A2BRKO) mice were kindly provided by Dr. Michael Blackburn (University of Texas, Houston, TX, USA). Male and female A2BR-KO mice were bred onto a C57BL/6 background (≥10 backcrosses) in the New York University School of Medicine Animal Facility. Mice described as wild type (WT) were all maintained on the C57BL/6 background by the breeder (Taconic Laboratories, Albany, NY). Protocols for experimental procedures involving the use of animals were approved by the New York University School of Medicine Institutional Animal Care and Use Committee.

Mouse bone sample preparation

After sacrifice, both hind legs were excised from WT and A2BRKO mice (four animals for each group). Left hind limbs, assigned to immunohistochemistry analysis, were cleaned of soft tissue, placed into 4 % PFA for 48 h, and decalcified in 10 % EDTA for 4 weeks.

Paraffin-embedded histological sections (5 μm) were cut, mounted, and prepared for analysis with TRAP staining as previously described [8]. In order to count the osteoblast number, immunohistochemistry was performed by using osteopontin antibody. Briefly, joint sections were deparaffinized by xylene and re-hydrated in decreasing ethanol concentrations. Slides were incubated for 15 min in an antigen retrieval solution (0.6 units/ml of proteinase K in TE buffer). Sections were deprived of endogenous peroxidase activity with 3 % H_2O_2 in methanol, then blocked with PBST containing bovine serum albumin (1 %) and FBS (5 %) for 60 min. Sections were incubated overnight with Rb-osteopontin antibody (1:200). After rinsing with phosphate-buffered saline (PBS), horseradish peroxidase (HRP)-conjugated secondary antibody was applied (1:200) for 1 h and stained with diaminobenzidine (DAB). Slides were scanned using the Leica microscope equipped with Slidepath Digital Image Hub version 3.0 Software.

Microcomputed tomography (μCT)

Right hind limbs from mice were disarticulated and used for morphology and measurement of the bone features. After fixation in 70 % ethanol, femora and tibiae of each sample were scanned with a SKYSCAN-1172 instrument and analyzed for bone parameters. Briefly, serial 12.5-μm tomographic images were acquired at the condition of 70 kV and 113 mA. Constant thresholds (200) were performed in binary images to segment bone from bone marrow. 2D and 3D images were obtained and the region of interest (ROI) in trabecular subchondral and distal bone was defined as a sclerotic area contouring from the bone surface above the growth plate.

In vivo bone formation

In order to highlight differences in bone formation, the calcein–Alizarin Red assay was performed in 6- and 12-week-old A2BRKO mice and in WT mice at the same age. Mice were injected with calcein (10 mg/kg, i.p.) in 2 % NaHCO3. After 7 days, mice were injected with Alizarin Red (35 mg/kg, i.p.). Mice were sacrificed after 2 days from the last injection. Both legs were harvested and fixed for 48 h in PFA 4 %. After washing with PBS, the samples were transferred into 15 % sucrose overnight and then into 30 % sucrose for 3 h. Samples were embedded in OCT before slide preparation.

Table 1 μCT analysis of subchondral bone. μCT analysis of the hind paws was carried out as described in "Material and methods." Data are expressed as mean ± SEM of four animals for each group which was then analyzed by two-way ANOVA and Bonferroni post hoc test

	Age (weeks)	GENOT.	BV/TV		BMD		Tb Th		Tb N	
Femur	6	WT	32.42 ± 0.91	*p* value = 0.089	0.3365 ± 0.010	*p* value = 0.250	0.060 ± 0.001	*p* value = 0.579	5.41 ± 0.071	*p* value = *0.002*
		A2BRKO	27.88 ± 2.02		0.3054 ± 0.022		0.059 ± 0.004		4.85 ± 0.078	
	12	WT	34.40 ± 2.14	*p* value = 0.598	0.3924 ± 0.010	*p* value = *0.015*	0.065 ± 0.002	*p* value = 0.377	5.25 ± 0.093	*p* value = *0.038*
		A2BRKO	32.84 ± 0.63		0.357 ± 0.009		0.064 ± 0.001		4.95 ± 0.067	
	19	WT	36.07 ± 1.94	*p* value = 0.743	0.3868 ± 0.019	*p* value = 0.883	0.069 ± 0.002	*p* value = 0.657	5.00 ± 0.110	*p* value = 0.081
		A2BRKO	37.06 ± 2.14		0.3989 ± 0.019		0.073 ± 0.004		4.76 ± 0.040	
Tibia	6	WT	35.93 ± 0.69	*p* value = *0.017*	0.3695 ± 0.004	*p* value = 0.082	0.059 ± 0.006	*p* value = 0.833	6.01 ± 0.126	*p* value = *0.002*
		A2BRKO	30.23 ± 1.59		0.3268 ± 0.020		0.0590.004		5.15 ± 0.118	
	12	WT	38.23 ± 1.71	*p* value = *0.035*	0.3979 ± 0.015	*p* value = *0.016*	0.065 ± 0.002	*p* value = 0.8407	5.73 ± 0.215	*p* value = *0.032*
		A2BRKO	31.27 ± 1.91		0.3382 ± 0.010		0.065 ± 0.001		4.94 ± 0.189	
	19	WT	35.77 ± 0.89	*p* value = 0.502	0.3900 ± 0.008	*p* value = 0.577	0.069 ± 0.002	*p* value = 0.984	5.17 ± 0.218	*p* value = 0.435
		A2BRKO	34.37 ± 1.74		0.4048 ± 0.024		0.069 ± 0.003		4.94 ± 0.082	

Italicized numbers indicate values with a statistically significant p-value

Osteoclast differentiation and PIT formation assay

After sacrifice, the long bones were excised and all the muscle was removed. The epiphyses were cut off and the bone marrow was flushed out using a syringe with a 27 gauge needle with α-MEM containing 1 % Penicillin/Streptomycin/10 % FBS. The cells were separated by using a pipette and left in the incubator overnight. The day after, only the floating cells were collected, centrifuged, and cultured with α-MEM containing 1 % P/S, 10 % FBS, and 30 ng/ml of MCSF. After 3 days, the cells that were not attached were removed and the media was replaced with α-MEM containing RANKL 50 ng/ml. The media with new RANKL was changed every 2 days. Osteoclast differentiation was tested by using TRAP staining, as previously described [6] and by gene expression analysis by using RT-PCR. To evaluate the expression of macrophages and osteoclast markers in A2BRKO and WT osteoclast, RNA was extracted after 7 days of differentiation. RNA extraction was performed using RNeasy Mini Kit (Qiagen, Invitrogen) and QIAshredder columns (Qiagen, Invitrogen), following the manufacturer's protocol. RNA reverse transcription was performed using the MuLV Reverse Transcriptase PCR Kit (Applied Biosystems). After RNA reverse transcription to cDNA, real-time PCR reactions were performed for a relative quantification of ADGRE and Cathepsin K performed on a Stratagene Mx3005P (Agilent Technologies, CA,

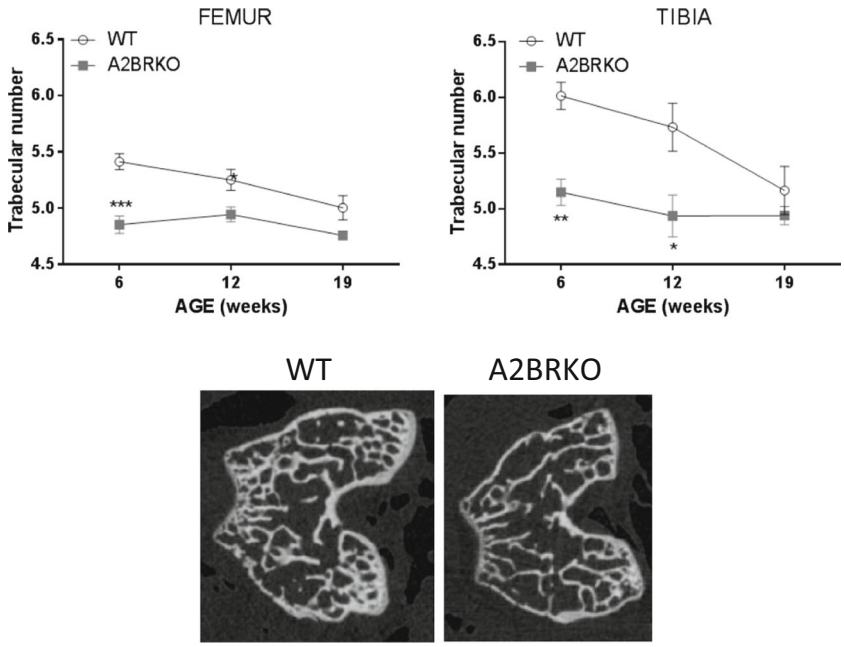

Fig. 1 There is a decrease in the trabecular number in the subchondral bone of A2BRKO mice. Trabecular number was determined by μCT in 6, 12, and 19-week-old WT and A2BRKO mice. Plotted in the two graphs are the mean trabecular number in femur and tibia of WT and A2BRKO mice collected at different ages. Representative 2D images of subchondral femur of 6-week-old A2BRKO and WT mice. Data are expressed as mean ± SEM of four animals for each group and significance of differences was determined by two-way ANOVA and Bonferroni post hoc test; *$p < 0.05$; **$p < 0.01$; ***$p < 0.001$

Table 2 μCT analysis of distal bone. μCT analysis of the hind paws was carried out as described in "Material and methods." Data are expressed as mean ± SEM of four animals for each group which was then analyzed by two-way ANOVA and Bonferroni post hoc test

	Age (weeks)	GENOT.	BV/TV		BMD		Tb Th		Tb N	
Femur	6	WT	10.94 ± 0.7447	*p* value = *0.037*	0.144 ± 0.006	*p* value = 0.055	0.044 ± 0.001	*p* value = 0.815	2.493 ± 0.131	*p* value = *0.036*
		A2BRKO	7.97 ± 0.85		0.120 ± 0.008		0.044 ± 0.002		1.806 ± 0.218	
	12	WT	17.60 ± 2.67	*p* value = 0.093	0.020 ± 0.024	*p* value = 0.085	0.061 ± 0.005	*p* value = 0.073	2.823 ± 0.223	*p* value = 0.177
		A2BRKO	12.10 ± 1.41		0.155 ± 0.012		0.050 ± 0.002		2.388 ± 0.188	
	19	WT	11.94 ± 1.37	*p* value = *0.003*	0.149 ± 0.007	*p* value = 0.562	0.057 ± 0.003	*p* value = 0.276	2.091 ± 0.127	*p* value = *0.0001*
		A2BRKO	5.05 ± 0.25		0.155 ± 0.005		0.063 ± 0.004		0.812 ± 0.065	
Tibia	6	WT	7.28 ± 0.26	*p* value = 0.061	0.114 ± 0.002	*p* value = 0.088	0.041 ± 0.001	*p* value = 0.501	1.782 ± 0.063	*p* value = *0.015*
		A2BRKO	5.48 ± 0.74		0.098 ± 0.008		0.043 ± 0.004		1.259 ± 0.142	
	12	WT	13.6 ± 1.761	*p* value = 0.190	0.171 ± 0.017	*p* value = 0.215	0.055 ± 0.003	*p* value = 0.116	2.453 ± 0.199	*p* value = 0.544
		A2BRKO	10.40 ± 1.31		0.143 ± 0.013		0.049 ± 0.001		2.258 ± 0.229	
	19	WT	9.73 ± 0.97	*p* value = *0.0003*	0.123 ± 0.017	*p* value = 0.853	0.054 ± 0.003	*p* value = 0.157	1.780 ± 0.109	*p* value = *0.0001*
		A2BRKO	2.28 ± 0.31		0.127 ± 0.012		0.061 ± 0.002		0.385 ± 0.072	

Italicized numbers indicate values with a statistically significant p-value

USA) with Brilliant SYBR Green Kit QPCR Master Mix (Stratagene, Agilent Technologies, CA, USA), according to the manufacturer's protocol.

Osteoclast functionality was tested using the pit formation in dentin assay. For this assay, cells are cultured and differentiated on dentin slices. After 7 days, cells were removed by washing the slices with 50 % bleach for 10 min and the dentin discs were stained with 1 % Toluidine blue for 5 min. Resorption pits are visualized by light microscopy and resorption area was quantified using ImageJ software (NIH, Bethesda, MD) [14].

Osteoblast isolation and functionality assay

After removal of the bone marrow, the diaphysis was cut in small pieces (1–2 mm), washed with PBS and incubated in a solution containing 2 mg/ml of Collagenase II at 37 °C for 2 h. The bone was transferred in a flask containing complete culture medium (DMEM, 100 U/ml penicillin, 50 μg/ml streptomycin, 50 μg/ml gentamicin, 1.25 μg/ml amphotericin B, 100 μg/ml ascorbate, 10 % FBS). Bone cells start to migrate from the bone after 3–5 days. In order to test the osteoblast functionality, Alizarin Red, alkaline phosphatase, and Sirius Red staining were performed in osteoblast cultures from WT and A2BR-KO mice as previously described [15].

Data analysis

μCT analysis was performed using the software CT-Analyzer to calculate various bone characteristics (Bruker- Kontich, Belgium). Bioquant software (Nashville, TN) was used to count the number of

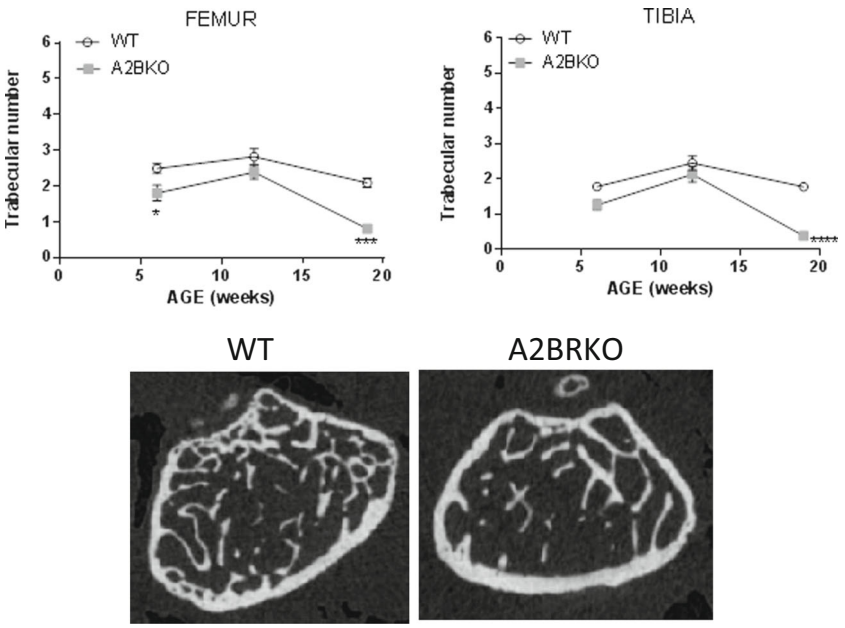

Fig. 2 There is a decrease in the trabecular number in distal bone of A2BRKO mice. Trabecular number was determined by μCT in 6, 12, and 19-week-old WT and A2BRKO mice. Plotted in the two graphs are the mean trabecular number in femur and tibia of WT and A2BRKO mice collected at different ages. Representative 2D images of distal femur of 19 weeks old A2BRKO and WT mice. Data are expressed as mean ± SEM of four animals for each group and significance of differences was determined by two-way ANOVA and Bonferroni post hoc test; *$p < 0.05$; ****$p < 0.001$

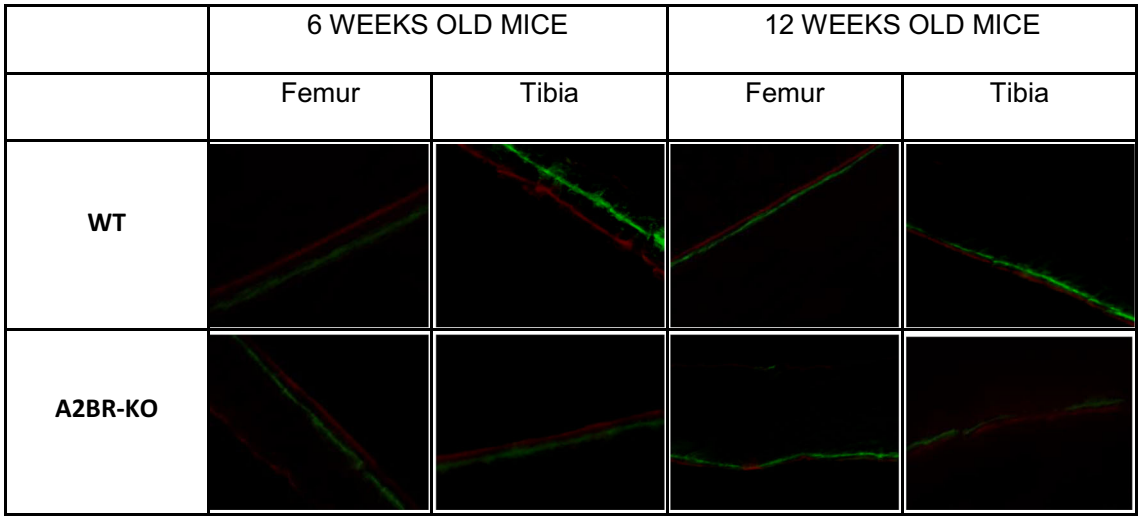

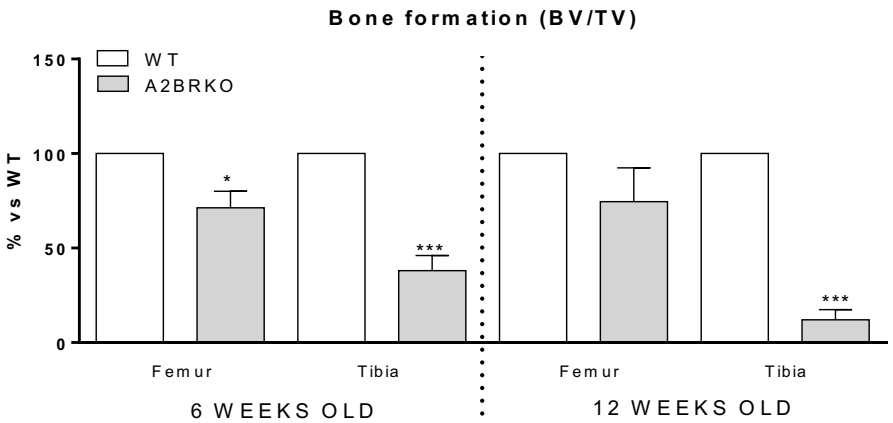

Fig. 3 A2BRKO mice have diminished bone formation in hind limbs. A2BRKO and WT mice (6 weeks old, $n = 5$) and adult (12 weeks old, $n = 5$) were injected with calcein and Alizarin Red, as described in "Material and methods." Shown are representative images of bone viewed under fluorescence microscopy. Below are plotted the mean (±SEM) % bone formation, measured as the distance between the red and green lines. A2BRKO mice show less bone formation compared to the WT mice at the same age. Data are expressed as mean ± SEM of five animals for each group (Student's *t* test: $*p < 0.05$; $***p < 0.001$)

osteoclasts and osteoblasts in relation to the total bone on the tissue slide and to measure the new bone formation. Statistical significance for differences between groups was determined using Student's *t* test, two-way or one-way ANOVA with Bonferroni post hoc test, as appropriate, using GraphPad software (GraphPad, San Diego, CA).

Results

μCT analysis of bone in A2BRKO mice

To determine whether bone develops normally in A2BRKO mice, we examined long bone structure in young (6 weeks old) and adult (12 and 19 weeks old) mice by μCT. We observed a decrease in the trabecular number in subchondral bone in both the femur and tibia of A2BRKO mice at 6 (in femur and tibia) and 12 weeks (in tibia) of age as compared to WT mice (Table 1 and Fig. 1). We also observed a decrease in bone mineral density in tibias of A2BRKO mice. More marked differences were noted between A2BRKO mice and WT mice with a marked decrease in bone substance (bone volume/total volume and trabecular number) in both the femur and tibia in 19-week-old mice. Similar results were found in the distal bone (Table 2 and Fig. 2).

Effect of A2BR deletion on bone formation

Because A2BR have previously been reported to play a role in promoting bone formation by cultured osteoblasts [3, 9–13], we determined whether deletion of A2BR affected bone formation in vivo. Following serial injection of fluorescent markers deposited at sites of new bone formation, we observed that A2BRKO mice produced

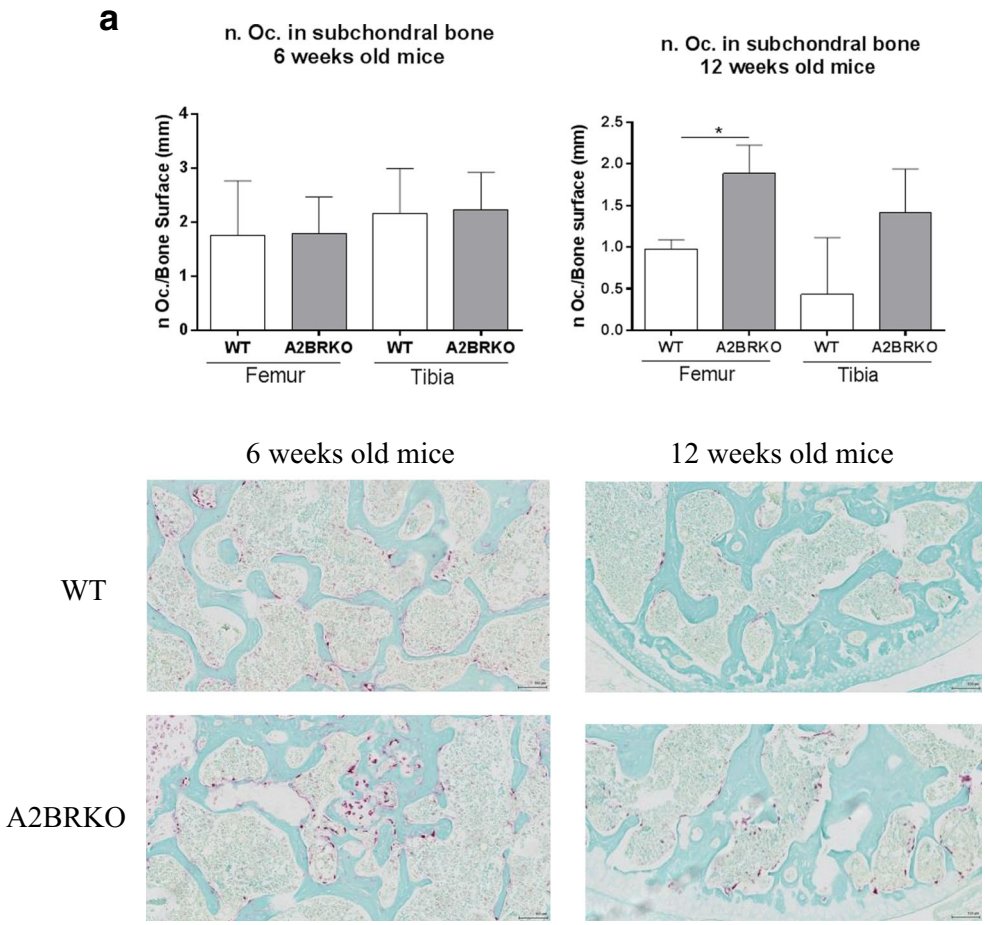

Fig. 4 There are more osteoclasts in bone of A2BRKO mice- Following decalcification of bone and paraffin embedding sections were stained for TRAP+ cells, as described in "Material and methods" and the number of TRAP+ cells/hpf was determined. **a** Representative images of subchondral femoral bone stained with TRAP are shown on the *bottom of the graphs* and plotted are the number of osteoclasts per bone surface in subchondral bone of 6- and 12-week-old mice. **b** Representative images of distal bone and the number of osteoclasts/area of bone is shown. Data are expressed as the mean ± SEM ($n = 4$ for each group; Student's t test: $^{*}p < 0.05$; $^{**}p < 0.01$)

significantly less bone in the femur (71 % vs WT mice) and tibia (38 % vs WT mice) of 6-week-old mice. Moreover, new bone formation was reduced in the tibia of adult A2BRKO mice as well (Fig. 3), consistent with the changes in bone detected by microCT.

Effect of A2BR deletion on bone resorption

We have previously reported that A2BR stimulation suppresses osteoclast differentiation [3], so we next sought to determine whether deletion of A2BR leads to an increase in osteoclasts, as seen in A2ARKO mice [6]. We observed that there was a marked increase in TRAP-positive osteoclasts on the surface of bone in both subchondral femur and distal tibia of 12 weeks old A2BRKO. Similarly, there were more osteoclasts in the midshaft femur of young A2BRKO mice (Fig. 4a, b) as well.

In vitro osteoclast differentiation and functionality

To determine whether the increase in osteoclast number in bone of A2BRKO mice was due to increased capacity of individual cells to differentiate into osteoclasts or from altered expression of signals for osteoclast differentiation, we studied RANKL-induced differentiation of osteoclasts from A2BRKO mice in vitro. We observed increased RANKL-induced osteoclast differentiation in ex vivo cultured bone marrow cells from A2BRKO mice as compared to those isolated from WT mice (21 ± 8 vs 63 ± 16 osteoclasts/well, WT vs A2BKO, respectively, $p < 0.05$). Increased RANKL-induced osteoclast differentiation in A2BRKO cells was confirmed by real-time RT-PCR analysis; expression of ADGRE, a specific macrophage marker, was decreased, and the osteoclast marker Cathepsin K was increased in A2BRKO bone marrow cells following RANKL stimulation, as compared to marrow from WT mice. Moreover, there was a 344 % increase in pit

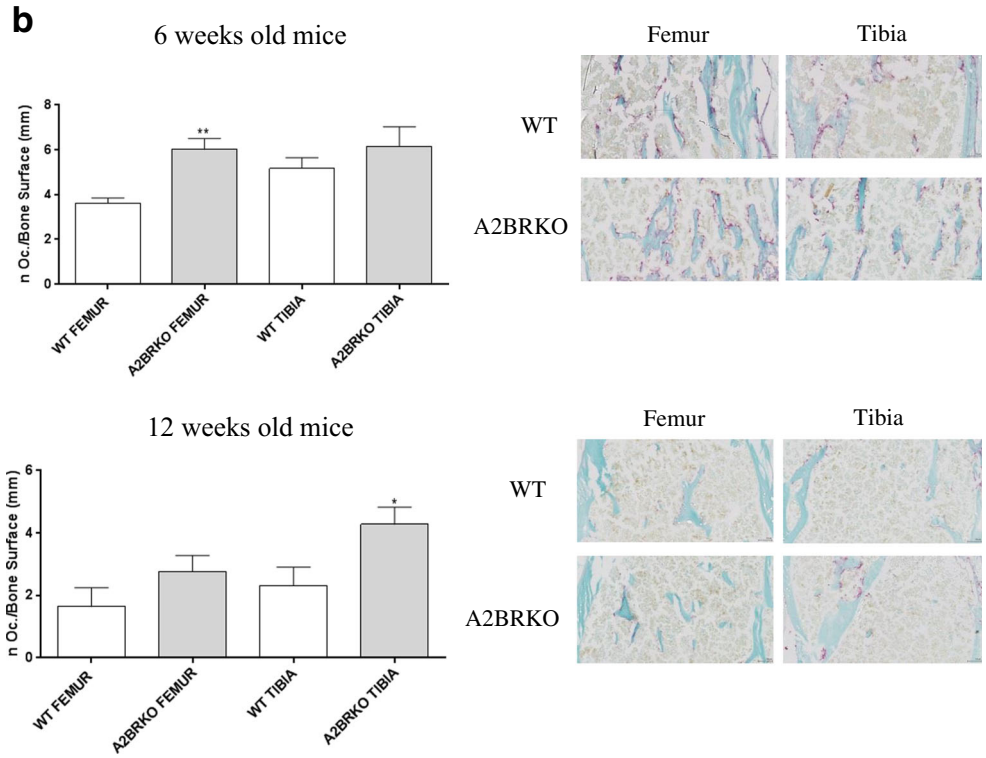

Fig. 4 continued.

formation by A2BRKO osteoclasts cultured on dentin as compared to those from WT mice (Fig. 5).

Ex vivo osteoblast differentiation and functionality

There were 32 % fewer osteoblasts in the tibias of 6-week-old A2BRKO mice than in tibias from WT mice (Fig. 6). By 12 weeks of age, this difference was no longer significant. Moreover, there was no difference in the number of osteoblasts in the femurs at either 6 or 12 weeks of age (Fig. 6). Surprisingly, the osteoblasts cultured from the bone of A2BRKO mice expressed more alkaline phosphatase (145 % of those from WT mice) and deposited more calcium, as detected by Alizarin Red staining (174 % vs WT), and collagen deposition, as detected by Sirius Red staining (176 % of WT osteoblasts, Fig. 7a–c).

Discussion

Bone is a highly dynamic structure that is constantly undergoing remodeling; there is tight coupling between bone formation and breakdown in the adult skeleton [16]. We and others have extensively studied the role of adenosine and its receptors, in particular A1 and A2A receptors in the maintenance of bone homeostasis in both in vivo and in vitro systems, in rodent and human cells [2–8]. A recent report suggests that adenosine plays little direct role in regulating or maintaining bone homeostasis, based primarily on in vitro studies [17]. This report is clearly inconsistent with both our prior reports and those of others based on both in vitro and in vivo studies [1–8, 10, 11, 13, 14, 18]. It is likely that the source of the cells studied (calvarial vs. trabecular bone) may be responsible for the observed differences, although other studies indicate that both A1AR and A2AR stimulation can induce regeneration of calvarial bone in mice [8, 19]. Prior studies have demonstrated a role for A2BR in promoting osteoblast differentiation and inhibiting osteoclast formation and function and in bone healing [3, 9–13]. In the studies reported here, we provide evidence that further confirms that A2BR play a role in regulating bone homeostasis. The principal effect of A2BR deletion in mice is loss of trabecular bone in long bones. The μCT analysis revealed a general decrease of bone in hind paws of A2BRKO mice. Prior work had shown a decrease of bone in the distal metaphysis of 4-week-old mice that was not found in older mice (8 weeks and 15 weeks old [9]). In our studies, the A2BRKO mice manifested an osteopenic phenotype in the subchondral bone until 12 weeks of age but the osteopenic phenotype of the midshaft bone was more persistent in the older mice. These findings underline the regional differences in bone formation that occur at different times of life. The regional differences in the effects of A2BR deletion on bone formation and remodeling are

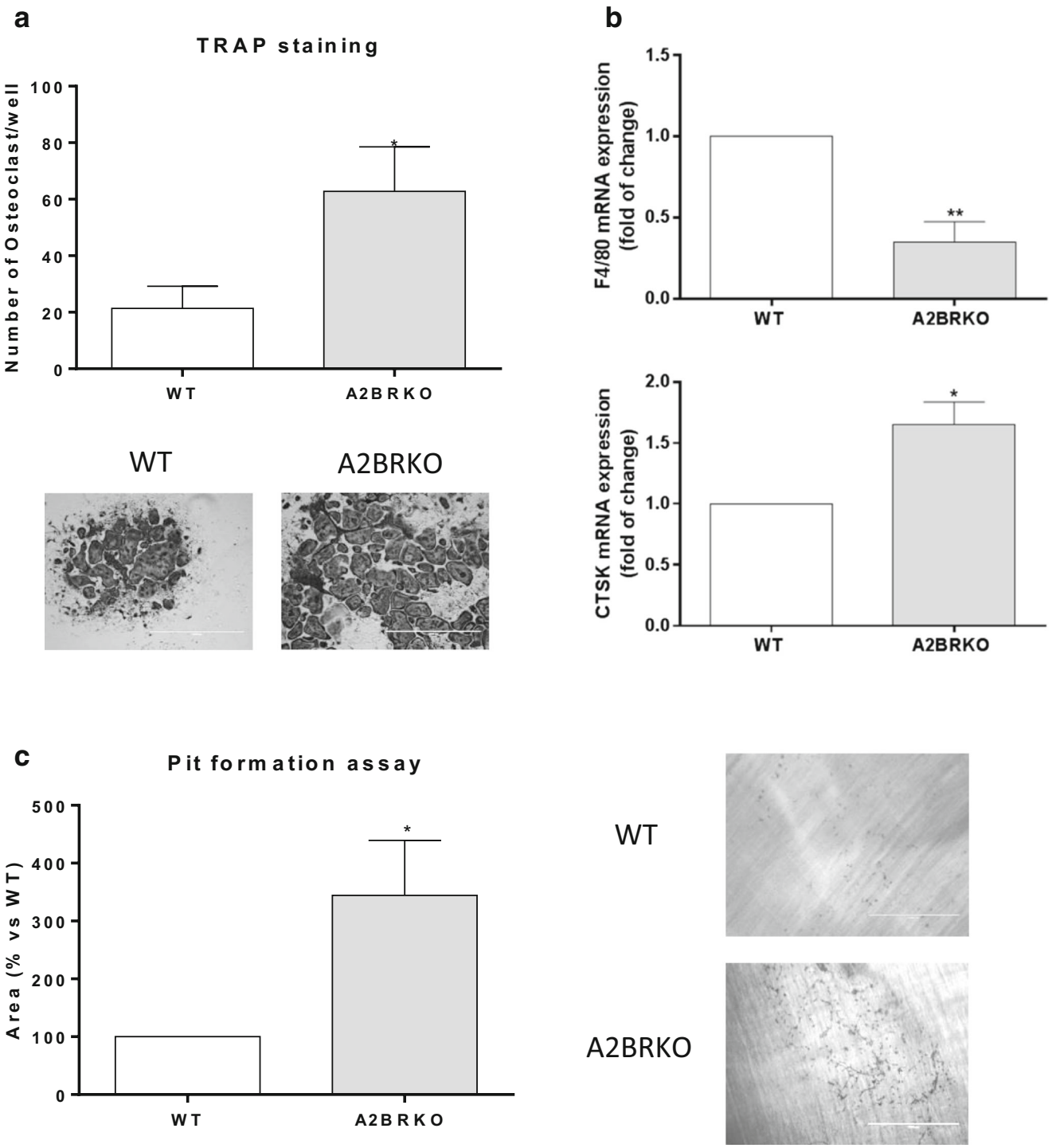

Fig. 5 Increased differentiation and functionality of A2BRKO osteoclasts—more bone marrow-derived osteoclast precursors from A2BRKO mice differentiate into osteoclasts in response to M-CSF/RANKL than from precursors isolated from WT mice (**a**; $n = 4$ experiments performed in duplicate) with a decrease in gene expression for ADGRE (F4/80, a macrophage marker) and an increase for Cathepsin K gene expression (**b**; $n = 3$ experiments performed in duplicate). **c** A2BRKO osteoclasts also degrade more dentin than osteoclasts from WT mice. Data are expressed as mean ± SEM (Student's t test: $^{*}p < 0.05$; $^{**}p < 0.01$)

striking. An increase of osteoclast number was detected in the subchondral and midshaft bone and a decrease of osteoblasts only in the subchondral tibiae of young mice. Regional differences in bone loss are seen after menopause in women and the risk of fracture is much more marked in the hip, femur, and vertebrae even though bone loss is observed more diffusely. The factor(s) governing these differences are not well understood and,

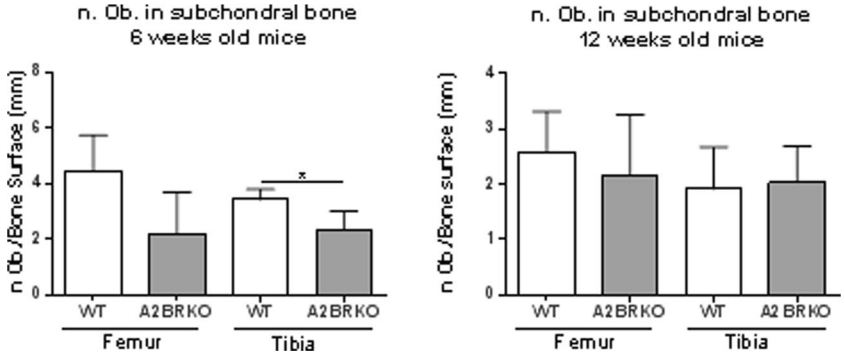

Fig. 6 There are fewer osteoblasts in the bone of A2BRKO mice—immunohistochemical staining of alkaline phosphatase as a marker of osteoblasts was carried out as described in "Material and methods." The number of osteoblasts was then counted in the tibias of 6-week-old A2BRKO and WT mice. Data are expressed as mean ± SEM ($n = 4$ for each group; Student's t test: $^{*}p < 0.05$)

similarly, the regional differences in the effect of A2BR deletion on bone phenotype are not understood.

Nonetheless, less is known about the effect of A2BR on bone production. We and others have previously demonstrated that pharmacological blockade of A2BR stimulation inhibits human osteoblast differentiation from human mesenchymal stem cells [3, 9]. Here we studied the A2BRKO mice during early adult life, from 6 to 19 weeks, and observed both their ability to form and maintain bone and the clear role of A2BR in regulating bone formation. Based on our prior demonstration that A2BR stimulation diminishes in vitro differentiation of osteoclasts, we were not surprised that there was increased osteoclast number in bone of A2BRKO mice and there was increased RANKL-induced osteoclast differentiation in vitro. Moreover, the reduction in osteoblast number in bone was not surprising although the apparent enhancement of function of the osteoblasts that had differentiated in vivo and were studied ex vivo was striking and likely represents a compensatory change. This finding explains the more modest bone phenotype observed in the A2BRKO mice than, for example, the A2ARKO mice in which there is more marked and diffuse osteopenia associated with enhanced osteoclast formation and

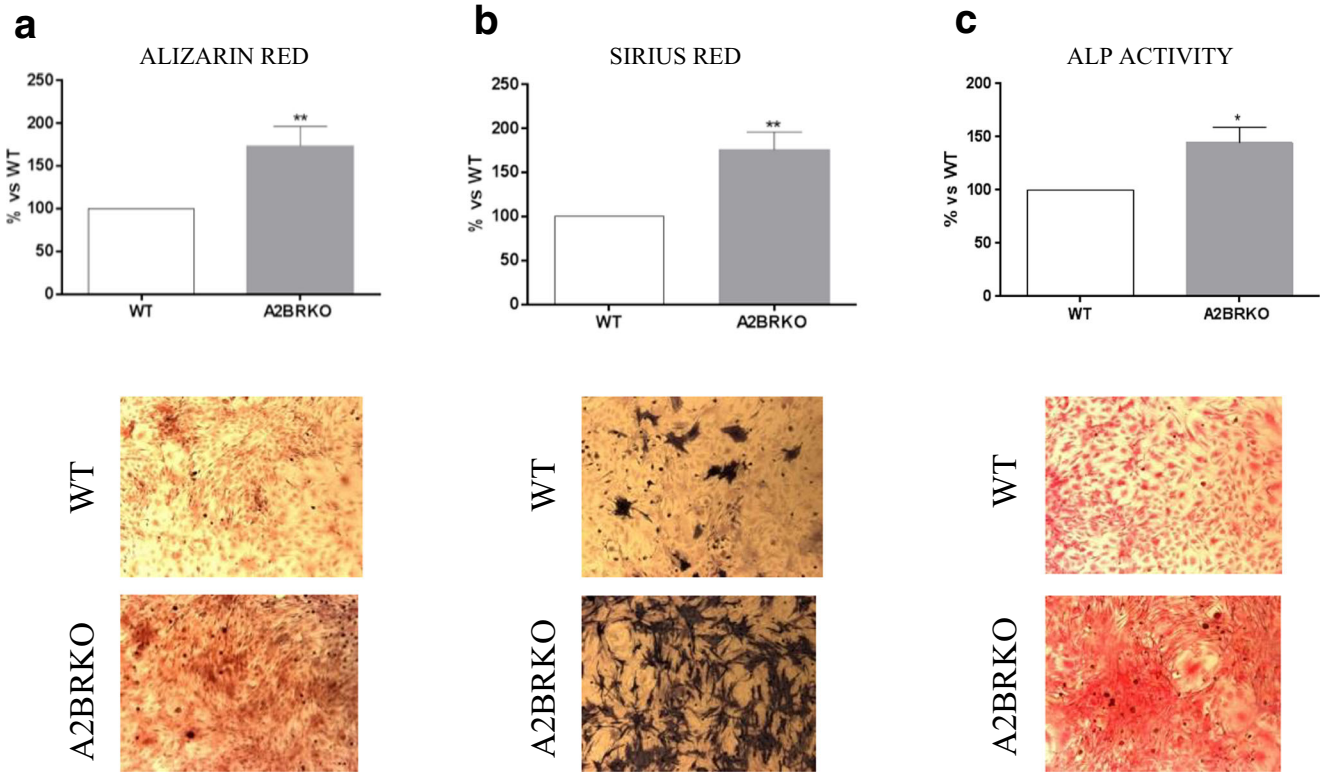

Fig. 7 Mature osteoblasts isolated from A2BRKO mice produce more calcified matrix, collagen, and alkaline phosphatase than osteoblasts isolated from WT mice—mature osteoblasts were isolated from the long bones of A2BRKO and WT mice, cultured and then stained for **a** calcified matrix production (Alizarin Red); **b** collagen deposition (Sirius Red); and **c** alkaline phosphatase activity ($n = 4$ experiments performed in duplicate). Data are expressed as mean ± SEM (Student's t test: $^{*}p < 0.05$; $^{**}p < 0.01$)

function and apparently reduced bone formation by mature osteoblasts in the absence of A2AR stimulation [3, 6, 8, 17].

The effect of A2BR in osteoclast reduction may be due to interference with NF-kB signaling resulting from an increase in intracellular cAMP. Our lab previously showed that the activation of A2AR or treatment with cAMP analogues reduces osteoclast formation and NF-kB nuclear translocation [7]. Because it is likely that A2BR limits the RANKL-RANK activation of NF-kB and loss of this "brake" on osteoclast differentiation contributes to the osteopenia observed in A2BRKO mice, it is likely that Denosumab, an agent that blocks osteoclast differentiation by inhibiting RANK activation, would prevent the bone loss in A2BRKO mice.

We observed clear suppression of osteoblast differentiation in the bones of mice lacking the A2BR, consistent with the prior observation that there is diminished in vitro differentiation of osteoblasts from A2BRKO precursors. Nonetheless, we were surprised to find that the osteoblasts that do differentiate in the A2BRKO mice are hyperactive and, at least, in part, are able to compensate for the reduced number of osteoblasts present. Previous studies indicate that stimulation of A2BR increases IL-6 expression and secretion in osteoblasts and other cell types [18–20] and IL-6 is known to affect osteoblast differentiation and function in a complex manner at different points during osteoblast differentiation and function [21]. Thus, reduction of endogenous IL-6 production in the A2BKO mice may underlie the diminished number of osteoblasts but apparent increase in function of the remaining osteoblasts. Similarly, A2BR stimulation reduces osteoblast expression of osteoprotegerin, a decoy receptor for RANKL that regulates osteoclast differentiation [20]. Thus, it is possible that diminished regulation of osteoclast differentiation by A2BRKO osteoblasts contributes to the increase in osteoclast number. Thus, we conclude that the complex effects of A2BR stimulation on bone homeostasis are responsible for the variable effects of A2BR loss on bone homeostasis in different loci and at different timepoints in the lifespan of A2BR-deficient mice.

The role of the A2BR in diseases of bone has not been well explored. Studies throughout the years and in multiple populations suggest that coffee ingestion is associated with accelerated postmenopausal bone loss and osteoporosis [22–26]. Caffeine, one of the principal active agents in coffee, is a non-selective adenosine receptor antagonist and blockade of A2B receptors by caffeine could contribute to the effect of coffee on bone health. Prior work by Carroll and co-workers suggests that A2BRKO mice heal fractures more slowly than wild type mice, as one might predict from the phenotypes of A2BRKO mice seen here and in prior studies [9]. Thus, it is likely that A2BR play a positive role in maintaining bone health.

Acknowledgments This work was supported by grants from the National Institutes of Health (5R01AR068593-02), Clinical and Translational Science Institute (1UL1TR001445-01).

References

1. Mediero A, Cronstein BN (2013) Adenosine and bone metabolism. Trends Endocrinol Metab 24(6):290–300
2. He W, Cronstein BN (2012) Adenosine A1 receptor regulates osteoclast formation by altering TRAF6/TAK1 signaling. Purinergic Signal 8(2):327–337
3. He W et al (2013) Adenosine regulates bone metabolism via A1, A2A, and A2B receptors in bone marrow cells from normal humans and patients with multiple myeloma. FASEB J 27(9):3446–3454
4. He W, Wilder T, Cronstein BN (2013) Rolofylline, an adenosine A1 receptor antagonist, inhibits osteoclast differentiation as an inverse agonist. Br J Pharmacol 170(6):1167–1176
5. Mediero A et al (2012) Adenosine A2A receptor activation prevents wear particle-induced osteolysis. Sci Transl Med 4(135): 135ra65
6. Mediero A et al (2012) Adenosine A(2A) receptor ligation inhibits osteoclast formation. Am J Pathol 180(2):775–786
7. Mediero A, Perez-Aso M, Cronstein BN (2013) Activation of adenosine A(2A) receptor reduces osteoclast formation via PKA- and ERK1/2-mediated suppression of NFkappaB nuclear translocation. Br J Pharmacol 169(6):1372–1388
8. Mediero A et al (2015) Direct or indirect stimulation of adenosine A2A receptors enhances bone regeneration as well as bone morphogenetic protein-2. FASEB J 29(4):1577–1590
9. Carroll SH et al (2012) A2B adenosine receptor promotes mesenchymal stem cell differentiation to osteoblasts and bone formation in vivo. J Biol Chem 287(19):15718–15727
10. Takedachi M et al (2012) CD73-generated adenosine promotes osteoblast differentiation. J Cell Physiol 227(6):2622–2631
11. Ciciarello M et al (2013) Extracellular purines promote the differentiation of human bone marrow-derived mesenchymal stem cells to the osteogenic and adipogenic lineages. Stem Cells Dev 22(7): 1097–1111
12. Trincavelli ML et al (2014) Osteoblast differentiation and survival: a role for A2B adenosine receptor allosteric modulators. Biochim Biophys Acta 1843(12):2957–2966
13. Kang H, Shih YR, Varghese S (2015) Biomineralized matrices dominate soluble cues to direct osteogenic differentiation of human mesenchymal stem cells through adenosine signaling. Biomacromolecules 16(3):1050–1061
14. Kara FM et al (2010) Adenosine A1 receptors (A1Rs) play a critical role in osteoclast formation and function. FASEB J 24(7):2325–2333
15. Bakker AD, Klein-Nulend J (2012) Osteoblast isolation from murine calvaria and long bones. Methods Mol Biol 816:19–29
16. Raggatt LJ, Partridge NC (2010) Cellular and molecular mechanisms of bone remodeling. J Biol Chem 285(33):25103–25108
17. Noronha-Matos J.B., Correia-de-Sa P. Mesenchymal stem cells ageing: targeting the "purinome" to promote osteogenic differentiation and bone repair. J Cell Physiol. 2016.
18. Wei W et al (2013) Blocking A2B adenosine receptor alleviates pathogenesis of experimental autoimmune encephalomyelitis via inhibition of IL-6 production and Th17 differentiation. J Immunol 190(1):138–146

19. Volpini R et al (2003) Medicinal chemistry and pharmacology of A2B adenosine receptors. Curr Top Med Chem 3(4):427–443
20. Evans BA et al (2006) Human osteoblast precursors produce extracellular adenosine, which modulates their secretion of IL-6 and osteoprotegerin. J Bone Miner Res 21(2):228–236
21. Le Goff B et al (2010) Role for interleukin-6 in structural joint damage and systemic bone loss in rheumatoid arthritis. Joint Bone Spine 77(3):201–205
22. de Franca NA et al (2016) Dietary patterns and bone mineral density in Brazilian postmenopausal women with osteoporosis: a cross-sectional study. Eur J Clin Nutr 70(1):85–90
23. ToRo KOR (2013) A study of risk factors and T-score variability in Romanian women with postmenopausal osteoporosis. Iran J Public Health 42(12):1387–1397
24. Hallstrom H et al (2013) Long-term coffee consumption in relation to fracture risk and bone mineral density in women. Am J Epidemiol 178(6):898–909
25. Hallstrom H et al (2006) Coffee, tea and caffeine consumption in relation to osteoporotic fracture risk in a cohort of Swedish women. Osteoporos Int 17(7):1055–1064
26. Harris SS, Dawson-Hughes B (1994) Caffeine and bone loss in healthy postmenopausal women. Am J Clin Nutr 60(4):573–578